

## Effects of high activator content on fly ash-based geopolymers exposed to elevated temperatures

Omar A. Abdulkareem,

*School of Housing, Building and Planning (HBP), University Sains Malaysia (USM), 11800  
Penang, Malaysia,*

*Email: [abdulkareem@usm.my](mailto:abdulkareem@usm.my); [eng.omar83@yahoo.com](mailto:eng.omar83@yahoo.com)*

**Abstract:** This article reports the influence of high alkaline activator content on the compressive strength and microstructure characteristics of a fly ash (FA) geopolymer system after exposure to elevated temperatures of 400 °C, 600 °C, and 800 °C. The sequential changes in the geopolymer gel structure after exposure to elevated temperatures and their effects on the residual strength were investigated through scanning electron microscopy (SEM) and X-ray diffraction (XRD). The results show that the high strength of the FA geopolymers reduced after exposure to 400 °C and 600 °C and failed in return any strength after exposure to 800 °C. The SEM results showed that the high activator content generated large quantities of unreacted crystals composed mainly from silicate underwent viscous sintering process at range of temperatures of 600 °C to 800 °C, and swelling resulting in system failure. XRD results showed that the geopolymers exposed to 800 °C exhibited significant decomposition in the aluminosilicate phase and amorphous hump compared to unexposed pattern.

**Keywords:** Geopolymer, Alkaline activator, Elevated temperature, XRD, SEM, Microstructure properties.

### 1. Introduction

The production of ordinary Portland cement (OPC) is one of the industries that significantly contribute to carbon dioxide (CO<sub>2</sub>) emission during calcination of the OPC prime material. Hardjito & Rangan [1] reported that the production of 1 ton of OPC emits approximately 1 ton of CO<sub>2</sub> to the atmosphere because of calcination and fuel combustion, which mainly involves fossil fuel. The demand for new infrastructures and buildings has increased because of the continuous increase in the human population worldwide; thus, the construction technology is facing a huge environmental challenge of developing green construction materials (binders) in addition to OPC. Geopolymer material could act as a substitute for OPC when used in construction of civil infrastructure. In comparison with OPC, geopolymer materials can reduce CO<sub>2</sub> emission by 80%–90% [2] and exhibit better mechanical and durability properties [3–5]. The geopolymerization technology involves the alkaline activation of typical precursors to form an aluminosilicate gel structure through the polycondensation reaction at low temperatures; these precursors include metakaolin, fly ash (FA), slag, and rice husk ash, which contain abundant silica (SiO<sub>2</sub>) and alumina (Al<sub>2</sub>O<sub>3</sub>) [6,7]. In this technology, a green geopolymer binder (cement) prepared from waste materials, such as FA-based geopolymer, is beneficial to the environment because it diminishes waste quantities disposed in landfills. FA geopolymer materials exhibit high mechanical properties, low density, low water absorption, negligible shrinkage, and high chemical and fire resistance [8]. Given these properties, FA geopolymer materials are considered as an alternative to OPC particularly because they can reduce CO<sub>2</sub> emissions by 80% compared with OPC [1]. Previous studies reported that FA geopolymer concrete can achieve compressive strength higher than 60 MPa after thermal curing [9, 10]. This material also presents excellent durability to most aggressive acids [11] and can resist sulfate attacks better than OPC mortars in reinforcement steel [12–14]. FA, a by-product of pulverized coal combustion in thermal power plants, is primarily composed of silicon (SiO<sub>2</sub>), aluminum (Al<sub>2</sub>O<sub>3</sub>), iron (Fe<sub>2</sub>O<sub>3</sub>), and calcium (CaO) oxides, with less amounts of magnesium, potassium, sodium, titanium, and sulfur oxides [1]. Accordingly, a highly alkaline activator is required to dissolve the acidic oxides of FA; therefore, the usage of normal water in the activation process of a FA source is inappropriate. The common alkaline activator used to prepare FA geopolymers is a liquid combination of sodium hydroxide (NaOH) or potassium hydroxide (KOH) and sodium silicate (Na<sub>2</sub>SiO<sub>3</sub>) or potassium silicate (K<sub>2</sub>SiO<sub>3</sub>) [15–18]. Many studies used Na-based activators to prepare FA geopolymers because of their economic advantages [19–22]. The content and concentration of liquid alkaline activator play a fundamental role in the development of high-strength FA geopolymers at low temperatures [22]; these factors also determine the thermal durability or fire resistance of FA geopolymers exposed to temperatures higher than 100 °C. At low to moderate activator contents (liquid/solid ratios of 0.2–0.4), FA geopolymers exhibit low thermal shrinkage and good strength retention after exposure to temperatures up to 1,200 °C [15, 16, 23–25]. Kong & Sanjayan [16] studied the effect of elevated temperatures on the FA geopolymer paste, mortar and

concrete systems prepared by the alkali-activation of a FA source with alkaline mixture of  $\text{Na}_2\text{SiO}_3$  and 7 M KOH solution at liquid/solid ratios of 0.33. They reported an increasing in the compressive strength of 6.4 % after the FA geopolymer paste exposed to elevated temperature of 800 °C for 1 hour. Furthermore, they concluded that aggregate size of larger than 10 mm resulted in good strength performance before and after exposed to 800 °C. Bakharev [23] studied the thermal and microstructure properties of FA geopolymer paste materials prepared by the activation of two FA sources by alkaline activator mixture of NaOH,  $\text{Na}_2\text{SiO}_3$  and  $\text{K}_2\text{SiO}_3$  at liquid/solid ratios of 0.27-0.345. She reported a shrinkage cracking and strength loss after exposed to 800 °C, due to the dramatic increase in the mean pore size and high deterioration of the aluminosilicate gel. Rashad & Zeedan [24] examined the thermal properties and microstructure characterization of alkali-activated FA synthesized by the activation of a FA source with  $\text{Na}_2\text{SiO}_3$  at three liquid/solid ratios of 0.2, 0.3 and 0.4. They concluded that using liquid/solid ratios of 0.2 and 0.3 in the preparation of FA geopolymers enhanced the thermal performance and increased the residual strength after the exposure to elevated temperatures ranged of 200-1000 °C, unlike the specimens prepared with liquid/solid ratio of 0.4, which underwent high strength loss upon similar exposure.

Moreover, at relatively high activator contents (liquid/solid ratios  $> 0.4$ ), FA geopolymers undergo high thermal shrinkage and strength deterioration incessantly after exposure to varied elevated temperatures up to 800 °C [26]. Hence, the variation in the strength loss behavior is affected by the differences in the activator content; such differences may be related to the high rate of structural water evaporation at a high liquid/solid ratio and may result in high thermal shrinkage and strength loss. Recent studies [27, 28] reported that the unreacted or partially reacted silicate species of alkaline activators in the geopolymeric gel matrix significantly affect the thermal behavior of FA geopolymers exposed to elevated temperatures. Fernández-Jiménez et al., [29] addressed the thermal behavior of FA geopolymers after exposed to elevated temperatures of 400-1000 °C. They reported that the FA geopolymer underwent significant variation in mechanical strength behavior and microstructure characteristics compared to unexposed specimens, especially when the geopolymers exposed to 600 °C. They attributed these variations to the molten vitreous phase of the unreacted or partially reacted alkaline activator species that led to small variation in the original dimension of the geopolymer specimens exposed to 600 °C. Despite various studies conducted, limited information is available regarding the effect of high activator content (liquid/solid ratios  $> 0.4$ ) on the thermal behavior and phase composition of FA geopolymers subjected to varied high temperatures. Such information would be exceptionally useful for designing FA geopolymer materials for applications that requiring high thermal durability.

This study aims to evaluate the effect of high activator content on the strength development, microstructure, and phase composition of FA geopolymers before and after exposure to elevated temperatures of 400 °C, 600 °C, and 800 °C. The geopolymers were prepared with the selected activator/FA ratio of 0.60. The prepared geopolymers were used to determine the role of high activator content in the geopolymerization reaction and strength development of FA geopolymers exposed to high temperatures.

## 2. Experimental procedure

### 2.1. Source materials

FA was provided by the Manjung Power Station, Lumut, Perak, Malaysia. FA was stored under shade at ambient temperature and covered by a thin plastic layer to protect from ambient humidity and maintain clean powder. FA was analyzed prior to mixing, and its chemical composition was determined using X-ray fluorescence (Table 1). Table 1 illustrates that the  $\text{SiO}_2$  and  $\text{Al}_2\text{O}_3$  compounds dominated the chemical composition of about 60.83 % of the total FA mass with 13.73 % iron oxide ( $\text{Fe}_2\text{O}_3$ ) and 11.28 % CaO in the composition. Other oxide compounds of MgO,  $\text{P}_2\text{O}_5$ ,  $\text{Na}_2\text{O}$ ,  $\text{K}_2\text{O}$ ,  $\text{TiO}_2$  and MnO were also detected in minor compositions. The sum composition of the  $\text{SiO}_2$ ,  $\text{Al}_2\text{O}_3$ ,  $\text{Fe}_2\text{O}_3$  and CaO compounds in the FA was found to be 74.56 %, and thus the FA is classified as Class F according to ASTM C618 [30]. With a specific surface area of 0.463  $\text{m}^2/\text{g}$ , about 90 % of FA presented particle size smaller than 40  $\mu\text{m}$  as indicated in the particle size analysis results of Figure 1. Figure 2 presents the XRD diffractogram of the FA showing that the FA is mainly an amorphous material with the appearance of a typical broad hallow at 16 to 38 2 $\theta$ . However, the FA diffractogram is also contains some of crystalline phases of quartz ( $\text{SiO}_2$ ) at 21, 26.6 and 65 2 $\theta$ , mullite ( $3\text{Al}_2\text{O}_3 \cdot 2\text{SiO}_2$ ) at 17.1 and 28.3 2 $\theta$  and hematite ( $\text{Fe}_2\text{O}_3$ ) at 24, 35 and 41 2 $\theta$ .

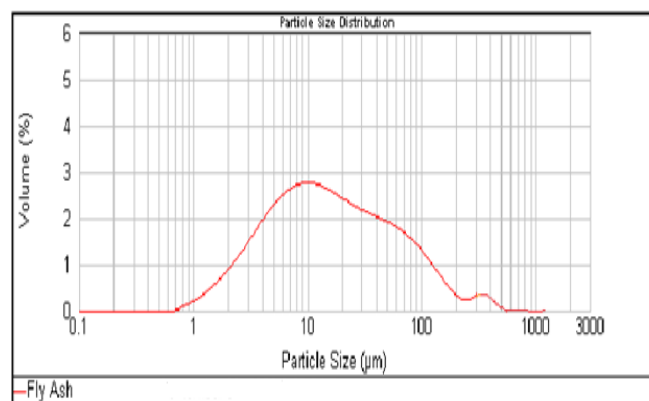
FA was activated with an alkaline activator, which was prepared by mixing technical-grade  $\text{Na}_2\text{SiO}_3$  (Sigma Chemical Ltd.) and NaOH solution. The chemical composition of  $\text{Na}_2\text{SiO}_3$  was 30.1%  $\text{SiO}_2$ , 9.4%  $\text{Na}_2\text{O}$ , and 60.5%  $\text{H}_2\text{O}$ , with a modulus ratio ( $M_S$ ) equal to 3.2 ( $M_S = \text{SiO}_2/\text{Na}_2\text{O}$ )

**Table 1.** Chemical composition of fly ash using (XRF) and the mix proportioning of the geopolymer paste.

Chemical	% By mass FA
SiO <sub>2</sub>	43.22
Al <sub>2</sub> O <sub>3</sub>	17.61
K <sub>2</sub> O	1.31
TiO <sub>2</sub>	0.88
MnO	0.14
CaO	11.28
Fe <sub>2</sub> O <sub>3</sub>	13.73
C	1.80
MgO	5.94
P <sub>2</sub> O <sub>5</sub>	0.87
Na <sub>2</sub> O	1.43
Loss on ignition (%)	1.80
FA (kg/m <sup>3</sup> )	341.89
Na <sub>2</sub> SiO <sub>3</sub> (kg/m <sup>3</sup> )	100.86
12M NaOH (kg/m <sup>3</sup> )	100.86
Na <sub>2</sub> SiO <sub>3</sub> /NaOH	1.00
Activator/FA mass ratio	0.60

## 2.2. Samples preparation and thermal exposure

FA geopolymer paste was prepared by mixing FA with the prepared alkaline activator (Na<sub>2</sub>SiO<sub>3</sub>/ NaOH = 1.00, 12 M NaOH) at a fixed mixing ratio of 0.60 (liquid/solid mass ratio) by using a 5-L capacity mixer for about 5 min. The mix proportioning of the geopolymer pastes is presented in Table 1. The mixture was poured into 100 mm × 100 mm × 100 mm cubic plastic molds. The fresh specimens were placed on a vibrator table for 2 min, and the molded specimens were wrapped using a thin plastic sheet to prevent water evaporation. The specimens were then cured in an oven at 70 °C for 24 hour after casting. After curing, the molds were removed from the oven and cooled at room temperature. The specimens were then demolded and stored under ambient conditions. After 27 days of aging, a number of the prepared specimens were further exposed to 400 °C, 600 °C, and 800 °C. The specimens were transferred into a furnace with a maximum heating temperature of 1,200 °C and then heated at a fixed heating rate of 4.4 °C/min to the targeted elevated temperatures. The geopolymer specimens were kept at each elevated temperature for 1 hour. Each specimen was cooled to room temperature inside the furnace. The unexposed specimens were left undisturbed under ambient condition for 28 days before testing their compressive strength. The compressive strength test for geopolymers exposed to elevated temperatures was performed 1 day after heating. All specimens (exposed and unexposed) were aged for 28 days.

**Figure 1.** Particle size distribution of the FA.

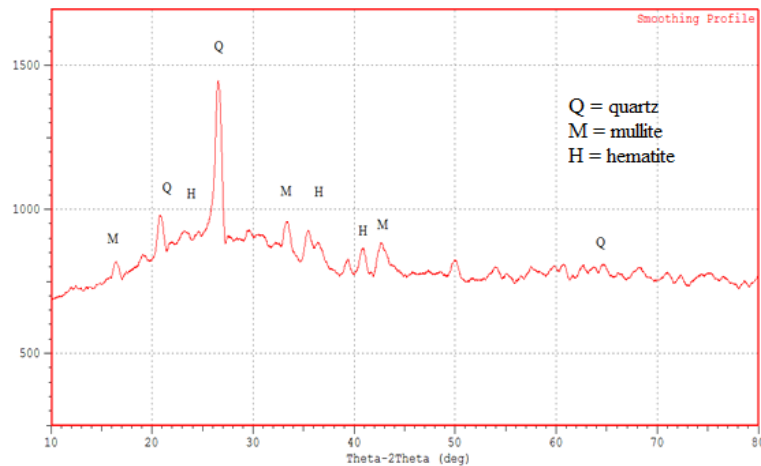


Figure 2. XRD diffraction pattern of the FA.

### 2.3. Compressive strength evaluation

The compressive strength of 100 mm × 100 mm × 100 mm specimens was tested according to EN 12390-3 [31]. The compression test was performed using a speed rate of 50 mm/min by using the Shimadzu Universal Testing Machine (Japan) with a maximum loading of 1,000 kN. A minimum of three specimens was tested to evaluate the compressive strength.

### 2.4. Microstructural investigation

#### 2.4.1. Scanning electron microscopy (SEM) measurements

The microstructures of the geopolymers unexposed and exposed to elevated temperatures were investigated through SEM using JSM-6460 LA Jeol (Japan). The specimen fragments were mounted in an epoxy resin, vacuumed, and coated with a thin platinum layer by using JFC-1600 auto-fine coater Jeol (Japan). The test was conducted using secondary electron detector. Energy-dispersive spectroscopy (EDS) was also performed to investigate the chemical composition of the selected spots in the obtained SEM micrographs.

#### 2.4.2. Phase composition investigation

X-ray diffraction (XRD) was performed to explore the phase composition and the crystalline content of the geopolymers unexposed and exposed to elevated temperatures by using XRD-6000 (Shimadzu, Japan). The samples were cut into small geopolymer slices and then ground into powder with sizes of 100-120 μm suitable for the test requirement. The test was performed under operating conditions of 40 kV and 30 mA with Cu-Kα wavelengths of 1.54060 and 1.54439 Å. For data collection, the 2θ increment was 0.02°, counting time step was 0.3 %/min, and 2θ range was 10° to 80°.

### 2.5. Thermogravimetric measurement

The mass loss with gradual temperature increase was measured for the geopolymer paste specimens using the thermogravimetric analysis (TGA). The TGA measurement was conducted using PerkinElmer, Pyris diamond thermogravimetric/differential thermal analyzer. Fragments of the geopolymer paste specimens used for strength test analysis were powdered and used in the TGA test to ensure the thermal equilibrium during transient heating is achieved.

## 3. Results and Discussion

### 3.1 Mechanical strength and thermogravimetric analysis

Table 2 shows the 28 days compressive strength, residual strength, and strength loss results of the geopolymer paste specimens cured at 70 °C and after exposure to 400 °C, 600 °C, and 800 °C. The initial compressive strength (44.83 MPa) of the unexposed geopolymer indicates that the geopolymerization reaction produces reacted and dense aluminosilicate gel structure owing to the high activator solution content (liquid/solid mass ratio = 0.60). However, the high strength of the resultant geopolymer sharply reduces after exposure to 400 °C and 600 °C, with strength losses of 38.2% and 56.5%, respectively, compared with the initial strength. Furthermore, the geopolymer exposed to 800 °C does not retain any residual strength (failed). The visual examination of the specimen exposed to 800 °C shows sharp and deep thermal cracks on the surface with significant swelling that causes extreme alteration in their original dimensions as illustrated in Figure 3. Moreover, the strength loss increases with temperature because of the thermal shrinkage caused by the

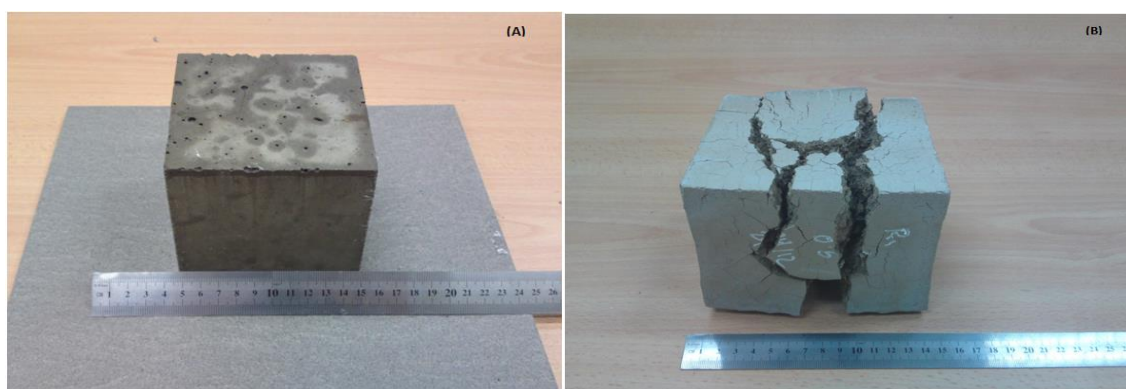
aggressive dispersion of the structural water from the geopolymer structure at high temperatures. Generally, the hardened geopolymer structure still contains some water content and hydroxyl groups, which are transformed to water vapor when the geopolymer is heated at temperature higher than 100 °C [31]. The vapor pressure continuously increases with heating temperature until it reaches the maximum limit; under this condition, the dense matrix with less permeability cannot restrain the high thermal stresses which leading to intensive thermal cracks on the specimen surfaces caused by thermal shrinkage. This phenomenon is known as “the vapor effect” [31].

Figure 4 shows the thermogravimetric analysis (TGA) and the derivative thermogravimetric analysis (DTG) curves for the geopolymer paste. These tests used for measuring the mass loss as a function of temperature from 25 °C to 800 °C. The TGA/DTG curves illustrate a sharp decrease in weight before 150 °C, attributed to the evaporation of both the free water and part of the chemically bonded water from the geopolymer. The sharp weight loss before 150 °C indicates that the free water contributed about 55-60 % of the total water content in the geopolymer structure, which evaporates before 100 °C. However, the mass loss rate stabilizes after 150 °C up to 780 °C. Consequently, no mass loss was detected between 780-800 °C and the average of the mass remaining after the geopolymer being heated to 800 °C was about 80 %.

Rickard et al., [28] reported that a portion of the activating solution remains unreacted or partially reacted during geopolymer formation. This portion is consisting mainly from silicate underwent viscous flow and swelling of the high silicate secondary phases within the range of 700 °C to 800 °C, that might lead to high thermal expansion of the geopolymer [26, 27]. Fernández-Jiménez et al., [29] reported a strength gaining for their FA geopolymers (prepared at liquid/Solid ratio = 0.29) after exposed to 600 °C. They associated this strength gaining to the viscous flow of the high silicate phases which possibly filled the fissures, cracks or flaws (resulted due to the thermal stresses) as it solidifies and thus led to increase the residual strength. In our work, the geopolymer paste exposed to 800 °C possibly undergoes severe viscous flow and swelling of the high silicate secondary phases due to the high alkaline activator content used in the preparation of the geopolymers (liquid/solid mass ratio= 0.60). Therefore, the damaged structure does not retain any residual strength after exposure to 800 °C due to significant thermal expansion. The SEM and EDS analysis performed on the exposed FA paste to elevated temperatures in the next section is justifying this behavior and correlated with the residual strength results.

**Table 2.** Strength results of the geopolymers before and after exposure to elevated temperatures.

Temperature (°C)	Compressive strength (MPa)	Strength loss (%)
Normal Temp.	44.83	-
400	27.69	38.2
600	19.47	56.5
800	0	100



**Figure 3.** Photograph of the FA geopolymer paste, exposed to 800 °C (A) as cured at 70 °C, (B) exposed to 800 °C.

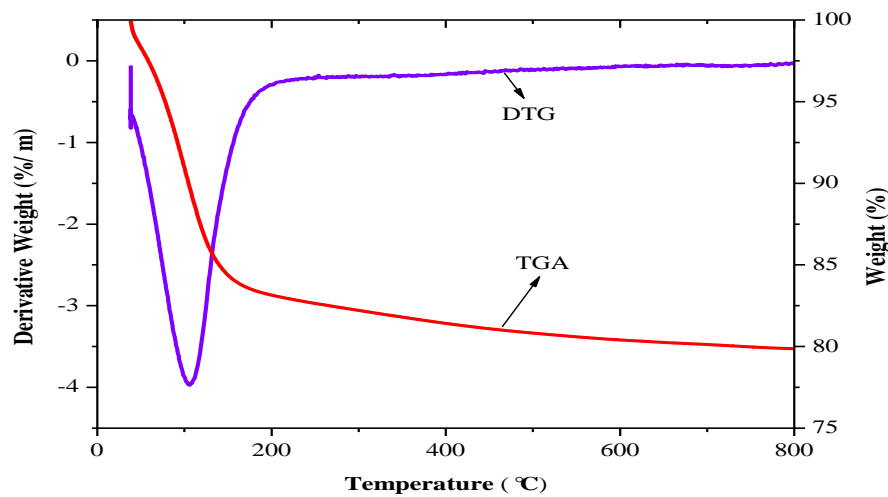
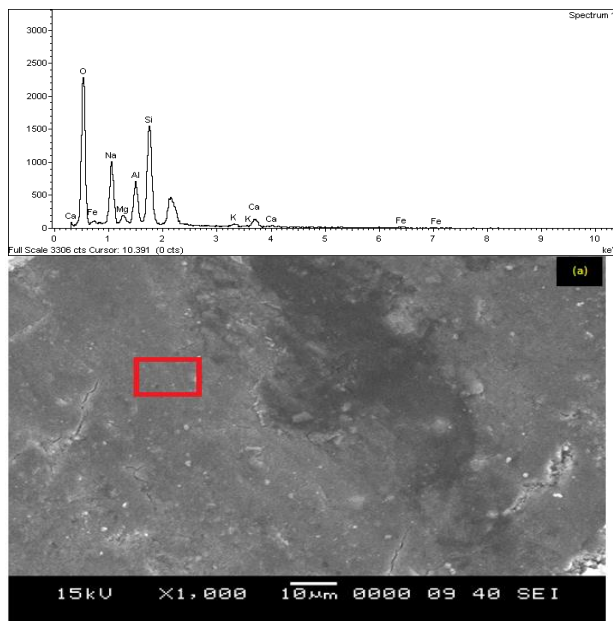


**Figure 4.** TGA and DTG curves of the FA geopolymer paste

### 3.2 SEM analysis

Investigations of the microstructure of the FA geopolymer paste using SEM shows significant changes in morphology as a result of exposure to the elevated temperatures. Figure 5 illustrates the SEM micrographs of the FA geopolymer pastes before and after exposure to the three elevated temperatures. Figure 5 illustrates that the microstructure of the unexposed geopolymer paste to elevated temperatures exhibits typical geopolymeric microstructure characteristics of dense and non-porous matrix consisting mainly of aluminosilicate gel as indicated by the EDS test quantitative analysis, signifying an effective geopolymerization reaction. Furthermore, the micrograph shows the absence of the unreacted FA microspheres, implying that the adoption of relatively high activator content may promote the high activation to FA and lead to produce high amount of geopolymeric products and initial compressive strength [7]. The microstructure contains small microcracks which are caused by the evaporation of water during curing and aging. In addition, the microstructure shows the presence of few bright crystals.



Element	Weight %	Atomic %	Compd %	Formula
Na K	11.69	10.96	15.75	Na <sub>2</sub> O
Mg K	1.42	1.26	2.35	MgO
Al K	8.84	6.26	16.81	Al <sub>2</sub> O <sub>3</sub>
Si K	23.21	17.81	49.66	SiO <sub>2</sub>
K K	1.41	0.78	1.70	K <sub>2</sub> O
Ca K	4.73	3.08	7.02	CaO
Fe L	4.99	2.31	6.71	FeO
O	42.71	57.54		
Totals	100.00			

**Figure 5.** SEM and EDS spot analysis for the FA geopolymers as cured at 70 °C.

Moreover, the initial matrix formed at 70 °C deteriorates when exposed to elevated temperatures. The microstructure of the geopolymer paste exposed to 400 °C (Figure 6) shows the development of microcracks. These features are due to the high water evaporation rate from the dense geopolymeric matrix; hence, the remaining microcracks and micro-pores in the matrix are responsible for the strength loss observed in Table 2. In

addition, exposure of the geopolymer paste to 400 °C increases the content of the bright crystals in the microcracks and pores (Figure 6). The geopolymer exposed to 600 °C exhibits further deterioration in the microstructure (Figure 7), as indicated by the further increase in the microcracks dimension and crystal content compared with the geopolymer paste exposed to 400 °C (Figure 6). The conducted EDS quantitative analysis shows that the crystals appeared in Figure 5c are composed of about 55 % of silicate. These silicate species are believed to be the excess activator solution portion that failed to react with the binder during the preparation and aging periods. These unreacted silicate crystals possibly undergo viscous flow and swelling resulting in extreme densification of the geopolymer paste structure after exposure to 800 °C as mentioned in section 3.1. Fernández-Jiménez et al., [29] reported that the excess activator solution exited in the FA geopolymer matrix as a dissolved portion in the aqueous phase of the material is responsible for the viscous flow at temperature higher than 600 °C.

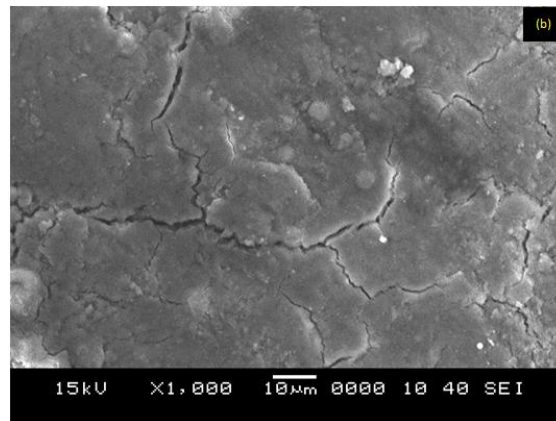
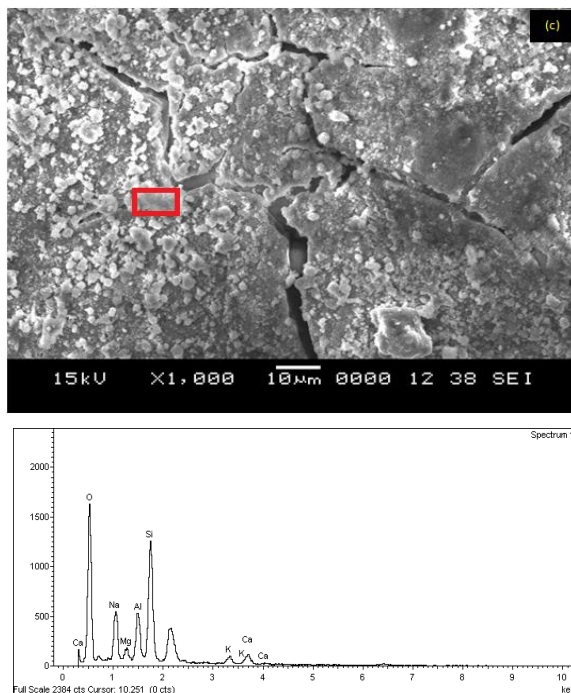


**Figure 6.** SEM and micrograph for the FA geopolymers exposed to 400 °C.



Element	Weight %	Atomic %	Compd %	Formula
Na K	8.86	8.11	11.94	Na <sub>2</sub> O
Mg K	2.04	1.76	3.38	MgO
Al K	8.26	7.44	16.60	Al <sub>2</sub> O <sub>3</sub>
Si K	26.08	19.55	55.79	SiO <sub>2</sub>
K K	4.27	1.30	5.14	K <sub>2</sub> O
Ca K	5.82	3.06	8.15	CaO
O	44.68	58.78		
Totals	100.00			

**Figure 7.** SEM and EDS spot analysis for the FA geopolymers exposed to 600 °C.

Further, Figure 8 demonstrates the severe deterioration in the microstructure morphology of the geopolymer paste exposed to 800 °C as shown by the evident destruction of the homogeneous aluminosilicate gel matrix formed at 70 °C. Therefore, the geopolymer paste exposed to 800 °C does not retain any residual strength because the excess activator content produced highly unreacted or partially reacted silicate materials; such materials appear as bright crystals in the SEM micrographs.

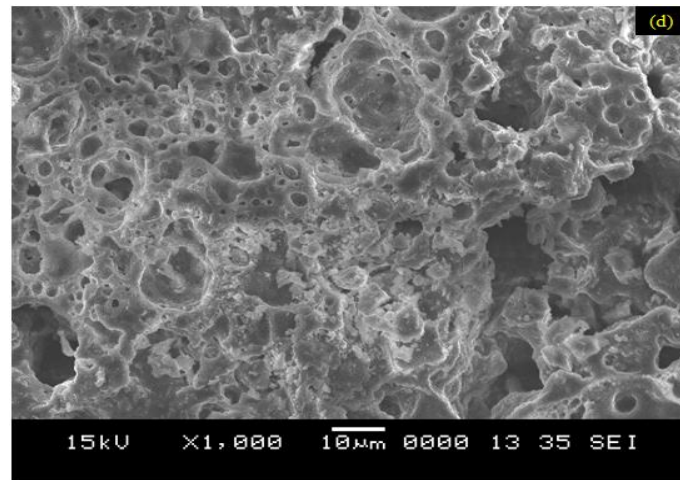


Figure 8. SEM and micrograph for the FA geopolymers exposed to 800 °C.

### 3.3. XRD analysis

Figures 9 to 11 illustrate the corresponding XRD patterns of the FA geopolymer pastes exposed to 400 °C, 600 °C, and 800 °C versus the XRD pattern of the unexposed FA geopolymer paste. The phase composition of the unexposed FA geopolymer paste shows a typical amorphous to semi-crystalline composition due to the existence of some crystalline traces of quartz ( $\text{SiO}_2$ ), mullite ( $\text{Al}_6\text{Si}_2\text{O}_{13}$ ), magnetite ( $\text{Fe}+2\text{Fe}_2+3\text{O}_2$ ), hematite ( $\text{Fe}_2\text{O}_3$ ), wollastonite ( $\text{CaSiO}_3$ ), aegirine [ $\text{NaFe}+3(\text{SiO}_3)_2$ ], calcium iron silicate ( $\text{CaFe}_3\text{O}_5$ ), and hercynite ( $\text{Fe}+2\text{Al}_2\text{O}_4$ ). The XRD pattern exhibits a broad hump, which is characteristic of an amorphous component. In addition, the phase composition of the unexposed geopolymers paste contains some zeolitic phases of hydroxysodalite ( $\text{Na}_4\text{Al}_3\text{Si}_3\text{O}_{12}\text{OH}$ ) and herschelite ( $\text{NaAl}-\text{Si}_2\text{O}_6\cdot 3\text{H}_2\text{O}$ ). These phases are difficult to observe in the XRD pattern because of their low peak intensities and excessive peaks overlapping with other phases. These zeolitic phases are attributed to the geopolymerization reaction of the FA source [32].

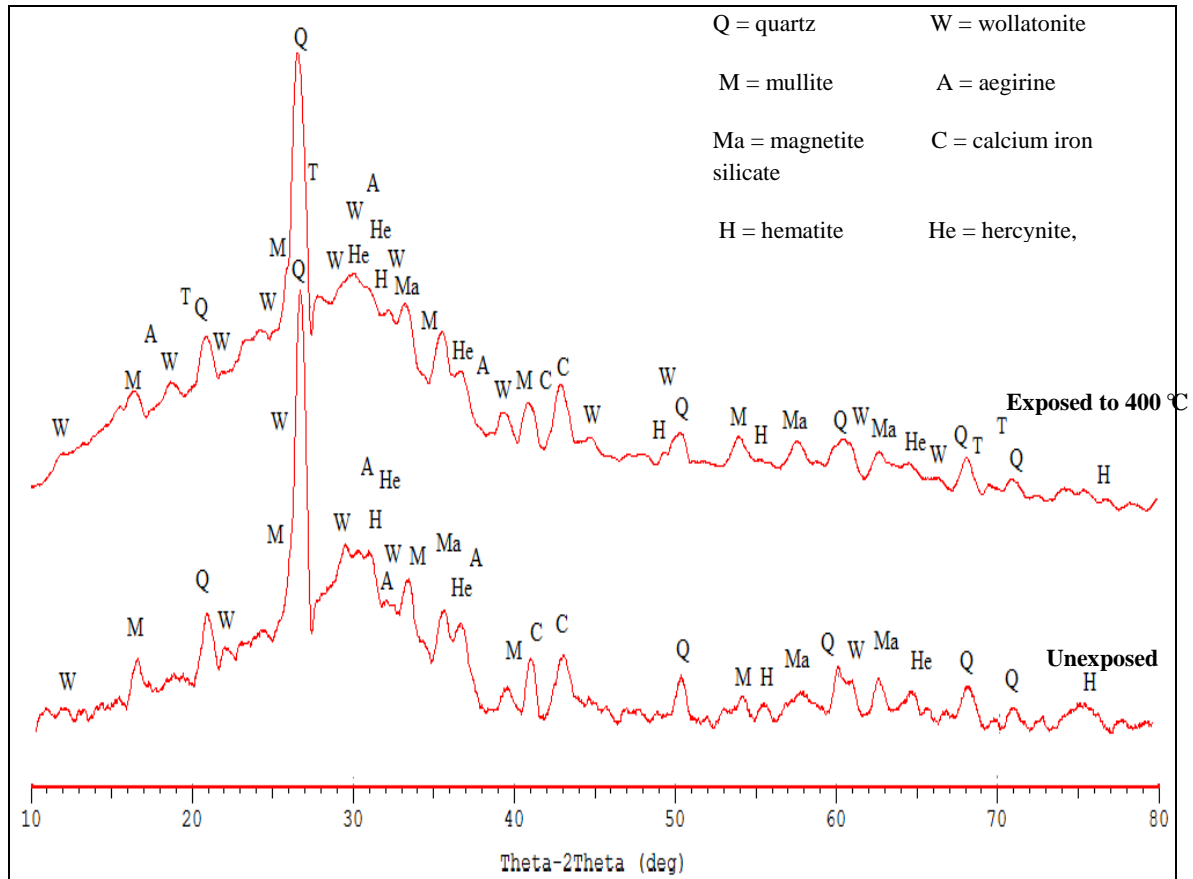
After exposure to the three elevated temperatures, the crystalline phase compositions of the exposed FA geopolymer pastes exhibit mild to significant changes compared with the unexposed FA geopolymer pastes. Figures 9 and 10 present the XRD patterns of the geopolymer pastes exposed to 400 °C and 600 °C versus the patterns of those unexposed, respectively. Several variations are observed in the crystalline phase after exposure to 400 °C and 600 °C, as indicated by the increasing iron oxide contents and peak intensities. The patterns of the geopolymers exposed to 400 °C and 600 °C also demonstrate the formation of other phases of tridymite ( $\text{SiO}_2$ ) and natrosilite ( $\text{Na}_2\text{Si}_2\text{O}_5$ ) particularly after exposure to 600 °C (Figure 10). In addition, the mullite and quartz peak intensities of the unexposed pattern decrease after heating to 400 °C and 600 °C, which are similar to the observations reported by Rickard et al., [28]. However, the geopolymers exposed to 400 °C and 600 °C retain their phase composition characteristics of the amorphous hump and other XRD major features of the unexposed FA geopolymer material. Figures 7 and 8 suggest that the geopolymers exposed to 400 °C and 600 °C undergo iron oxide phase changes, crystallization of the excess alkaline activator species, and partial destruction in the zeolitic phases composed of a high silicate content. These crystallized phases are believed to be detected in the form of white crystals in the SEM micrographs shown in Figures 6 to 8.

Figure 11 shows the significant changes in the phase composition of the FA geopolymer pastes exposed to 800 °C. For the exposed pattern, the Na-based feldspar phases of nepheline ( $\text{NaAlSiO}_4$ ) and albite ( $\text{NaAlSi}_3\text{O}_8$ ) are formed with high peak intensities with the presence of other original crystalline phases of the unexposed FA geopolymer. The formed phases of nepheline and tridymite improve the fire resistance of the geopolymers as indicated by their high melting points of 1,257 °C and 1,670 °C, respectively [28]. The bulk crystallization observed in the pattern for specimens exposed to 800 °C is caused by the free Na, Si, and Al species resulted from the decomposition of the zeolitic phases of the geopolymeric gel matrix. Similar observations have been reported by other authors [28, 29]. The geopolymer matrix contains also high amount of unreacted or partially reacted silicate species, and such species swell at range of temperatures of 600 °C to 800 °C caused extreme thermal expansion. This phenomenon is supported by the significant reduction and deterioration in the amorphous hump existed in the unexposed pattern after exposure to 800 °C (Figure 9). The presence of white crystals containing high silicate content also confirm this finding, as detected in the SEM and EDS results shown in Figures 6 to 8.

These results explain the failure of the FA geopolymer paste specimens to retain strength after exposure to 800 °C. Such reduction in the amorphous hump of the exposed FA geopolymer paste to 800 °C has not been reported by other phase studies on FA geopolymer pastes heated to 800 °C or 1,000 °C [24, 28, 29, 32, 33]. This



phenomenon could be due to the high alkaline activator content used in the preparation of the FA geopolymer specimen in this study, resulting in the formation of high content of unreacted silicate compounds. The presented thermal behavior of geopolymer at elevated temperatures indicates the significant effect of the liquid/solid mass ratio on the geopolymer performance at high temperature. Although the high activator content formed highly reacted and dense aluminosilicate matrix at 70 °C, the high portion of the unreacted silicate products significantly weakens the fire resistance of the geopolymer after exposure from 600 °C to 800 °C.



**Figure 9.** XRD diffraction patterns of the unexposed and exposed FA geopolymer paste to 400 °C.

#### 4. Conclusions

The following conclusions are established in this paper:

1) The relatively high activator content (liquid/solid ratio of 0.60) resulted in high compressive strength of 44.83 MPa for the FA geopolymer material. The high strength was caused by the high content of the geopolymerization reaction products in the formed geopolymeric matrix. However, after exposure to 400 °C and 600 °C, the strength significantly decreased with the corresponding strength losses of 38.2 % and 56.5 % because of the vapor effect phenomenon

2) The geopolymers exposed to 800 °C exhibited a strength loss of 100 % due to the swelling of the high silicate secondary phases resulted from the adoption of the relatively high activator content in the activation process of FA.

3) The SEM results presented the formation of a highly reacted dense aluminosilicate gel matrix at 70 °C. However, the formed matrix contained unreacted silicate-based crystals detected through EDS; such crystals significantly weakened the fire resistance of the geopolymers exposed from 600 °C to 800 °C due to mentioned swelling processes.

4) The XRD patterns of the geopolymers exposed to 400 °C and 600 °C manifested some changes in the crystalline phase in the form of increasing iron oxide contents. The patterns also presented the formation of silicate-based compounds particularly when the geopolymer was exposed to 600 °C.

5) The XRD results also showed significant reduction and deterioration in the amorphous hump existed in the unexposed specimens after exposure to 800 °C. The deterioration of the amorphous geopolymeric gel matrix was due to the high contents of the unreacted or partially reacted silicate species that swelled from 600 °C to 800 °C.

These observations elucidated the severe deterioration in the geopolymer paste structures and their failure to retain strength after exposure to 800 °C.

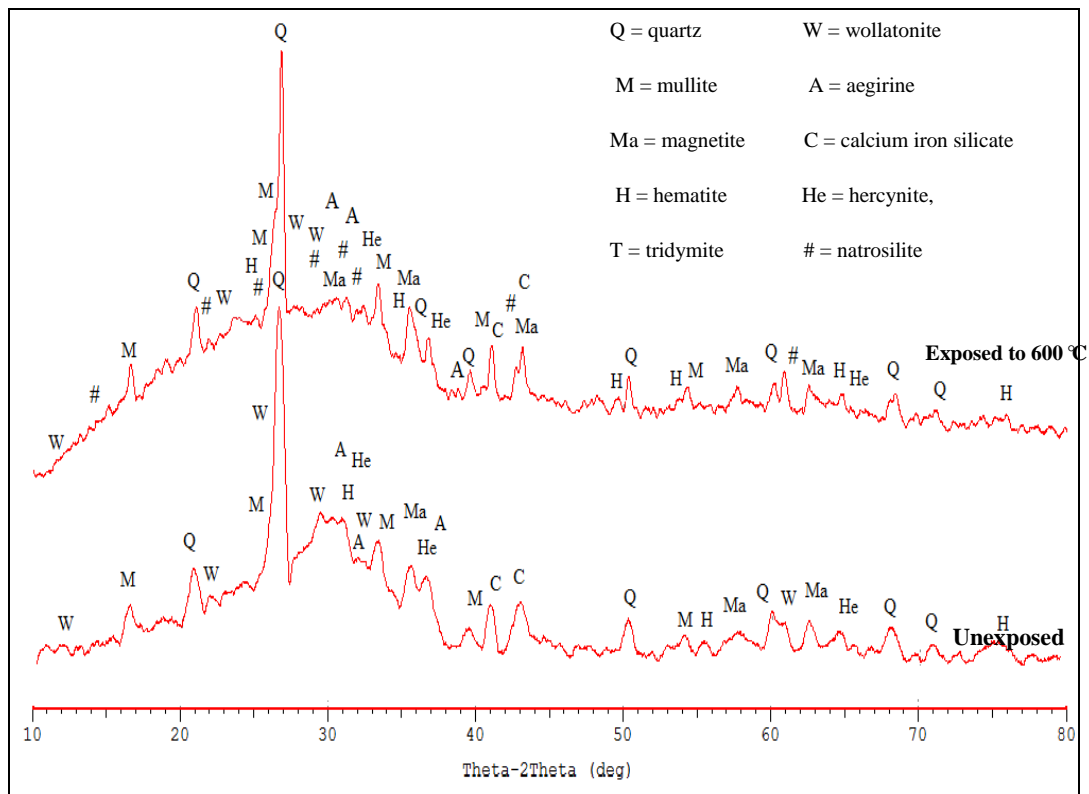


Figure 10. XRD diffraction patterns of the unexposed and exposed FA geopolymer paste to 600 °C.

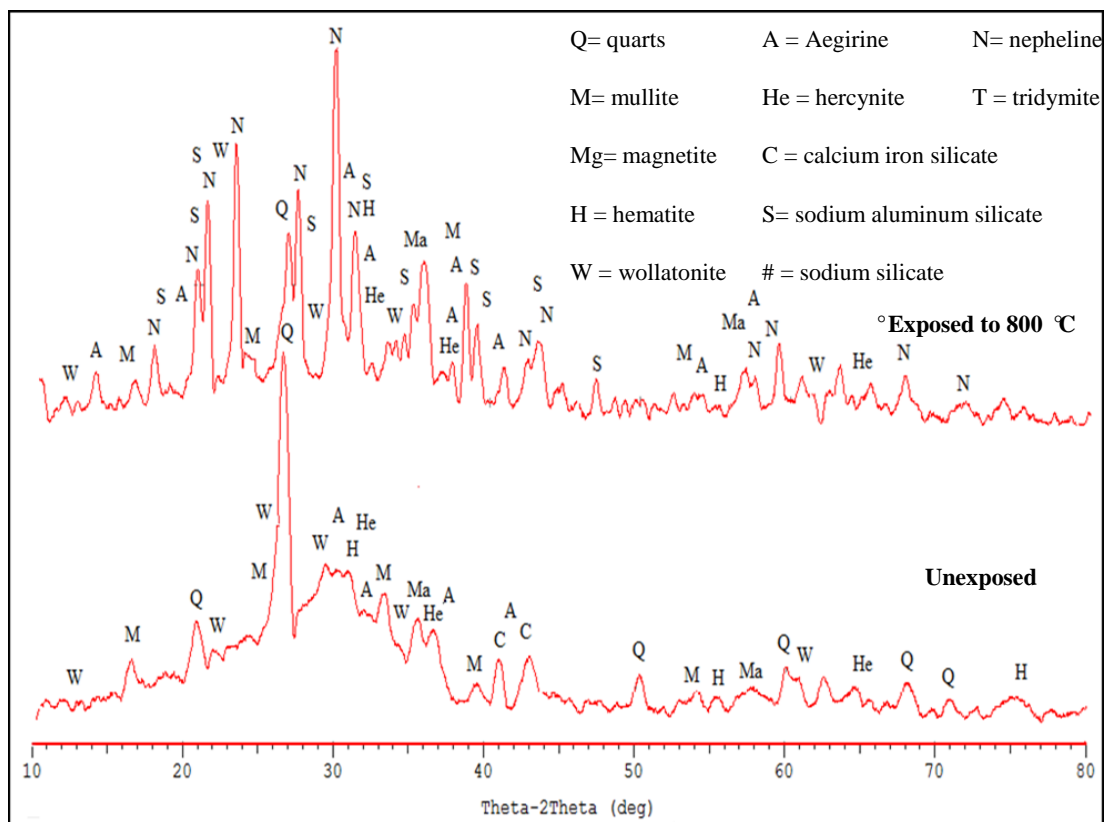


Figure 11. XRD diffraction patterns of the unexposed and exposed FA geopolymer paste to 800 °C.

## Acknowledgment

The author acknowledges the Malaysian Ministry of Higher Education and University Sains Malaysia (USM) for funding the study under the Fundamental Research Grant Scheme (203/PPBGN/6711347), Research University Grant (1001/PPBGN/814211) and Short Term Grant(304/PPBGN/6312106).

## References

- [1] Hardjito D, Rangan B V. Development and properties of Low-Calcium fly ash-based geopolymer concrete. Research report GC1, Curtin University of Technology, Australia (2005).
- [2] Davidovits J. Chemistry of geopolymeric systems, terminology. Proceedings of Second International Conference on Geopolymers, Saint- Quentin, France, 1999: 9–40.
- [3] Li, Z., Ding, Z., Zhang, Y. Development of sustainable cementitious materials in: International Workshop on Sustainable Development and Concrete Technology, edited by K. Wang, Beijing, China, May 20-21(2004).
- [4] Wallah, S., and Rangan, B. Low- calcium fly ash based geopolymer concrete: Long-term properties. *Research Report GC 2*, Curtin University of Technology, Perth, Australia, 2006: 97.
- [5] Gourley J., Johnson, G. Developments in geopolymer precast concrete. In: proceeding of fourth World Congress geopolymer, Geopolymer Institute, France. 2005: 133-137.
- [6] Duxson P. Fernandez-Jimenez A. Provis J L. Lukey G C, Palomo A. van Deventer JSJ. *Geopolymer technology: the current state of the art. Journal of Materials Science*. 2007; 42:17–2933. DOI: 10.1007/s10853-006-0637-z.
- [7] Detphan S., Chindaprasirt P. Preparation of fly ash and rice husk ash geopolymer. *International Journal of Minerals, Metallurgy and Materials*. 2009; 16: 720–726. DOI: 10.1016/S1674-4799(10)60019-2.
- [8] Thakur, R. N., & Ghosh, S. Effect of mix composition on compressive strength and microstructure of fly ash based geopolymer composites. *ARNP Journal of Engineering and Applied Sciences*, 2006; 4(4), 68-74.
- [9] Kovalchuk, G., Fernandez-Jimenez, A., & Palomo, A. Alkali-activated fly ash: Effect of thermal curing conditions on mechanical and microstructural development–Part II. *Fuel*. 2007; 86(3), 315-322. DOI: 10.1016/j.fuel.2006.07.010.
- [10] Duxson, P., Provis, J. L., Lukey, G. C., Mallicoat, S. W., Kriven, W. M., & Van Deventer, J. S. Understanding the relationship between geopolymer composition, microstructure and mechanical properties. *Colloids and Surfaces A: Physicochemical and Engineering Aspects*. 2005; 269(1), 47-58. DOI:10.1016/j.colsurfa.2005.06.060.
- [11] Fernandez-Jimenez, A., Garcia-Lodeiro, I., & Palomo, A. Durability of alkali-activated fly ash cementitious materials. *Journal of Materials Science*. 2007; 42(9), 3055-3065. DOI: 10.1007/s10853-006-0584-8.
- [12] Wallah, S., Hardjito, D., Sumajouw, D., & Rangan, B. Creep and Drying Shrinkage Behaviour of Fly Ash-Based Geopolymer Concrete. Proceedings from: The 22nd Biennial Conference Concrete. New South Wales, Australia. 2005:153-159.
- [13] Song, X., Marosszeky, M., Brungs, M., & Munn, R. Durability of fly ash based geopolymer concrete against sulphuric acid attack. Proceedings From: The 10<sup>th</sup> DBMC, International Conference on Durability of Building Materials and Components, Lyon, France. 2005: 123-129.
- [14] Fernandez-Jimenez, A. M., Palomo, A., Lopez-Hombrados, C. Engineering properties of alkali-activated fly ash concrete. *ACI Materials Journal*. 2006; 103(2), 106-112. DOI: 10.14359/15261.
- [15] Kong, D.L.Y & Sanjayan, J.G. Damage behavior of geopolymer composites exposed to elevated temperatures. *Cement and Concrete Composite*. 2008; 30, 986-991. DOI:10.1016/j.cemconcomp.2008.08.001.
- [16] Kong, D.L.Y. & Sanjayan, J.G. Effect of elevated temperatures on geopolymer paste, mortar and concrete. *Cement and Concrete Research*. 2010; 40,334-339. DOI:10.1016/j.cemconres.2009.10.017.
- [17]Rukzon, S., Chindaprasirt, P., Mahachai, R. Effect of grinding on chemical and physical properties of rice husk ash. *International Journal of Minerals, Metallurgy and Materials*. 2009; 16(2), 242-247. DOI: 10.1016/S1674-4799(09)60041-8.
- [18] Nazari, A., Riahi, S., Bagheri, A. Designing water resistant lightweight geopolymers produced from waste materials. *Materials and Design*. 2012; 35, 296-302. DOI:10.1016/j.matdes.2011.09.016.
- [19] Rashad, A. M. A comprehensive overview about the influence of different admixtures and additives on the properties of alkali-activated fly ash. *Materials and Design*. 2014; 35, 1005-1025. DOI: 10.1016/j.matdes.2013.07.074.
- [20]Temuujin, J., van Riessen, A, MacKenzie, K.J.D. Preparation and characterisation of fly ash based geopolymer mortars. *Construction and Building Materials*. 2010; 40, 1906–1910. DOI: 10.1016/j.conbuildmat.2010.04.012.
- [21] Nematollahi, B., Sanjayan, J. Effect of different superplasticizers and activator combinations on workability and strength of fly ash based geopolymer. *Materials and Design*. 2014; 57, 667-672. DOI: 10.1016/j.matdes.2014.01.064

- [22] Ryu, G. S., Lee, Y. B., Koh, K. T., Chung, Y. S. The mechanical properties of fly ash-based geopolymer concrete with alkaline activators. *Construction and Building Materials*. 2013; 47, 409–418. DOI: 10.1016/j.conbuildmat.2013.05.069.
- [23] Bakharev, T. Geopolymeric materials prepared using Class F fly ash and elevated temperature curing. *Cement and Concrete Research*. 2005; 35(6), 1224-1232. DOI:10.1016/j.cemconres.2004.06.031.
- [24] Rashad, A. M., & Zeedan, S. R. The effect of activator concentration on the residual strength of alkali-activated fly ash pastes subjected to thermal load. *Construction and Building Materials*. 2011; 25(7), 3098-3107. DOI:10.1016/j.conbuildmat.2010.12.044
- [25] Hussin, M. W., Bhutta, M. A. R., Ramadhansyah, P. J., Mirza, J., Azreen, M. Performance of blended ash geopolymer concrete at elevated temperatures. *Materials and Structures*. 2014; 48(3), 709-720. DOI.org/10.1617/s11527-014-0251-5.
- [26] Abdulkareem, O.A., Abdullah, M.M.A, Kamaruddin, H., Ismail, K., Binhussain, M. Mechanical and microstructural evaluations of lightweight aggregate geopolymer concrete before and after exposed to elevated temperatures. *Materials*. 2013; 6(10), 4450-4461. DOI: 10.3390/ma6104450.
- [27] Provis, J.L., Yong C.Z., Duxson P., van Deventer J.S.J. Correlating mechanical and thermal properties of sodium silicate-fly ash geopolymers. *Colloids and Surfaces A: Physicochemical and Engineering Aspects*. 2009; 336(1-3):57- 63. DOI:10.1016/j.colsurfa.2008.11.019.
- [28] Rickard W.D., Temuujin J., van Riessen A. Thermal analysis of geopolymer pastes synthesised from five fly ashes of variable composition. *Journal of Non-Crystalline Solids*. 2012; 358 (15): 1830-1839. DOI:10.1016/j.jnoncrysol.2012.05.032.
- [29] Fernandez-Jimenez A., Pastor J.Y., Marti A., & Palomo A. High-Temperature resistance in alkali-activated cement. *Journal of American ceramic Society*. 2010; 93 (10): 3411–3417. DOI: 10.1111/j.1551-2916.2010.03887.x.
- [30] ASTM C618-08a, Standard specification for coal fly ash and raw or calcined natural pozzolan for use in concrete. ASTM international; 2008.
- [31] Hu S., Wu J., Wen Y., HE Y., Fa-Zhou W., Qing-Jun D. Preparation and properties of geopolymer-lightweight aggregate refractory concrete. *Journal of Central South University of Technology*. 2009; 16(6): 914-918. DOI: 10.1007/s11771-009-0152-x.
- [32] Bakharev, T. Thermal behaviour of geopolymers prepared using class F fly ash and elevated temperature curing. *Cement and Concrete Research*. 2006; 36(6), 1134-1147. doi:10.1016/j.cemconres.2006.03.022.
- [33] Rickard, W. D., van Riessen, A., Walls, P. Thermal Character of Geopolymers Synthesized from Class F Fly Ash Containing High Concentrations of Iron and  $\alpha$ -Quartz. *International Journal of Applied Ceramic Technology*. 2010; 7(1), 81–88. DOI:10.1111/j.1744-7402.2008.02328.